

Effects of *Lactobacillus acidophilus* and *L. reuteri* on bone mass and gut microbiota in ovariectomized mice

Jingchen Chen[#], Xianyin Liu^{#*}, Songbo Li^{*}, Jianwen Li, Guanjun Fang, Yaoxin Chen, Xiaoqian Zhang

Department of Orthopedics, Affiliated Dongguan Hospital, Southern Medical University (Dongguan People's Hospital) & Dongguan Key Laboratory of Basic, Clinical and Digital Research on Common Orthopedic Diseases, Dongguan, 523000, China

[#]These authors contributed equally to this work.

ARTICLE INFO

Original paper

Article history:

Received: March 25, 2023

Accepted: July 06, 2023

Published: September 30, 2023

Keywords:

Osteoporosis; *Lactobacillus acidophilus*; *Lactobacillus reuteri*; Probiotics; osteoclast; bacteria; gut

ABSTRACT

Lactobacillus acidophilus (LA) and *L. reuteri* (LR) are widely used as food additives or medications in our daily lives. In OVX mice, LA and LR have been proven to inhibit bone loss. This study set out to find out how *L. acidophilus* and *L. reuteri* affected the bone mass of OVX mice and the mechanisms that underlie such effects. Fifty C57BL/6J female mice aged 6 weeks were subjected to five different treatments: sham surgery (sham), OVX surgery (OVX), OVX+LR (OVX and *L. reuteri* fed), OVX+LA (OVX and *L. acidophilus* fed), OVX+LR+LA (OVX and both *L. reuteri* and *L. acidophilus* co-fed), respectively. OVX mice were reared in groups until 16 weeks of age. Serum samples were collected, and IL-1 β , IL-6, TNF- α , and OCN levels were determined by ELISA. Bilateral femur thin-layer scanning was performed utilizing a micro-CT scanner. The scanning area was the entire femur. The sample data for bone density were produced via 3D multi-model software after the scanning procedure. To examine the microbial composition and characteristics, Illumina high-throughput sequencing was performed on mice feces. Following probiotic feeding, OVX mice showed an increase in trabecular number and thickness, bone volume fraction, and a reduction in trabecular separation. Blood levels of IL-1 β , IL-6, and TNF- α substantially dropped. The observed Chao1 and ACE indexes increased significantly. Changes in intestinal microorganisms occurred in all groups of mice. The change of the index in the gut microbes may indicate that the bone mass of OVX mice is changing. In OVX mice, *Lactobacillus acidophilus* shares the same role as *L. reuteri* in preventing bone loss. There are precise principles governing the changes in gut microbial diversity, the richness of certain bacteria, and inflammatory factors in bone metabolism following the administration of *Lactobacillus acidophilus* or/and *L. reuteri*.

Doi: <http://dx.doi.org/10.14715/cmb/2023.69.9.7>

Copyright: © 2023 by the C.M.B. Association. All rights reserved.

Introduction

Osteoporosis is a systemic metabolic bone disease that causes bone mass loss and microstructural bone tissue degradation. Once fractures occur in patients with osteoporosis, not only do their medical expenses and quality of life take a severe impact, but disability and mortality rates are also high(1). In China, osteoporosis prevalence rises with age and is greater in women than in men(2). The diagnosis of osteoporosis in postmenopausal women is based on a bone mineral density lower than the mean value for women of this age group by 2.5 standard deviations (3). Therefore, searching for new methods to diagnose and treat osteoporosis is of great importance to society.

Extensive recent research has demonstrated a close association between human diseases and gut microbiota (GM)(4). Significant changes in intestinal microbes were observed in people with abnormal bone mass. The diversity and abundance of GM were shown to be lower in postmenopausal patients with osteoporosis in a study of gut microbes in this population. At all taxonomic levels, the structure of the composition and abundance of strains changed(5). In a study of elderly people aged > 60 years in

Wuhan, China, the number of OTUs and microorganisms was lower at all levels in the population with low bone density, and the abundance of species changed at all taxonomic levels(6). Intestinal microbial diversity in patients with primary osteoporosis was significantly higher than in normal bone mass populations(7). The patterns of microbial changes in the gut are both the same and different for each type of osteoporosis.

The impact of GM and its metabolites on bone health is known as the gut-bone axis(8). Studies have shown that GM can influence bone metabolism through its metabolites, regulation of nutrient absorption, and the body's immune system(9). Animal experiments remain the most potent means to explore the gut-bone axis fully. The mouse GM model is a more applied and mature research model at this stage(4).

The application of probiotics to combat osteoporosis has become a popular trend today. Probiotics can modulate the gut microbial structure by producing antimicrobial molecules and competitively inhibiting pathogens. Probiotics not only produce antitoxins, block toxin expression, and interfere with the host response to toxins, but also absorb toxins and immobilize them in the cell wall, thus redu-

* Corresponding author. Email: dgphlxy@126.com(Xianyin Liu) and imsongbo0184@sina.com(Songbo Li)

cing the absorption of toxins in the gut. Probiotics improve the function of intestinal epithelial cells, forming a protective barrier that inhibits the adhesion of pathogens and cell invasion. Probiotics can also influence the production of inflammatory factors through immunomodulation and produce neurotransmitters in other body organs(10-12). A review of 57 clinical trials showed that probiotics are safe even in immunodeficient adults (human immunodeficiency virus infections, critically ill patients, surgical procedures, and patients with autoimmune diseases) (13).

Animal studies involving ovariectomized (OVX) mice have shown that *Lactobacillus reuteri* (LR) can effectively prevent bone loss by modulating intestinal microbes and inflammatory factors. LR inhibits the OVX-induced increase in CD4+T cells in the bone marrow(14). Inflammatory factors released by lymphocytes were inhibited by RIP2, while the expression of the osteoblast factor MC3T3-E1 was enhanced(15). In OVX mice to which LR was applied, the expression of the osteoclast signaling pathway inflammatory factors TNF- α , Trap5, IL-1 β , RANKL, and IL-10 was reduced, and the levels of OPG, which inhibits osteoclast differentiation and activity, was increased(14, 16, 17). LR altered the microbial community in the gut of OVX mice(14). It reversed the reduced osteoblast activity and increased osteoclast activity due to intestinal ecological dysregulation(18). A significant increase in serum 25-hydroxyvitamin D was found in a randomized controlled trial after oral administration of LR(19). This is consistent with the results in mice(20). However, in another randomized, placebo-controlled, double-blind clinical experiment, the decreases in bone mass did not achieve statistical significance after 12 months of LR alone in elderly women with reduced bone density, although adverse effects were similar to those in the placebo group(21). Therefore, we still need to discover a proven, safe, and effective probiotic to prevent and treat osteoporosis and study more about how LR influences bone mineral density.

L. acidophilus (LA) is a short gram-positive bacillus initially isolated from the human gastrointestinal tract. It is widely used as a food additive or a medication in our daily lives. Dietary intake is a significant factor in the acquisition of LA in humans. LA can survive in bile and low pH environments and adhere to human colonic cells, producing antimicrobial effects and lactase activity. Consumption of LA in humans exhibits immune activation, anti-hypercholesterolemia, infection control, and improved lactose metabolism. Its specific effects include controlling serum cholesterol levels, strengthening the immune system, balancing intestinal microbiota, preventing infection by intestinal pathogens, treating irritable bowel syndrome, improving the way lactose is digested by patients who are lactose intolerant, and enhancing the absorption of minerals and vitamins(22, 23). It also reduces the release of inflammatory factors in rheumatoid arthritis(24). Furthermore, it plays a role in the treatment of stress-related psychiatric disorders(25).

No clear reports exist confirming the influence of LA on bone mass, bone metabolic factors, and intestinal microorganisms in OVX mice. Additionally, no study shows how the pattern of microorganisms in the intestines of OVX mice changes when LA and LR are used. This study set out to confirm the osteoprotective effect of LA on OVX mice, discover the pattern of intestinal microbial changes in OVX mice after applying LA and LR, and offer novel

approaches for diagnosing and treating postmenopausal osteoporosis.

Materials and Methods

Experimental subjects

Charles River (Beijing, China) provided fifty C57BL/6J female mice aged 6 weeks. Five groups of mice were established at random (sham group, OVX group, LR+OVX group, LA+OVX group, LR+LA+OVX group), ten mice per group, and five mice/cage rearing (Figure 1). The rearing environment was SPF, with constant ambient temperature and humidity 24/7. A strict 12-hour-light-dark cycle was followed, and daily records of water and food consumption were kept.

After two weeks of acclimatization rearing (8 weeks of age), food and drink were provided to the mice in the sham and OVX groups. In the LR+OVX group, mice were given food and drinking water that included LR, while mice in the LA+OVX group received food and drinking water that contained LA. The LR+LA+OVX group received food and drinking water that contained LR+LA (Figure 1). The mice were fed a Co60 irradiated experimental mice maintenance diet obtained from Synergy Medical Bioengineering. The drinking water was autoclaved tap water. LR (GDMCC1.614) and LA (GDMCC1.412) were purchased from the Guangdong Institute of Microbiology (Guangdong Microbiological Analysis and Testing Center). The bacterial solution was stored in a refrigerator at 4–8 degrees Celsius during delivery. The strains were exposed to 10⁹ CFU/ml of drinking water. Each afternoon, the water bottles were replaced. Three times every week, the strains' ability to survive in the water bottles was tested, and the concentration decreased by not less than 10⁸ CFU/ml within 24 hours. The concentration of the bacterial solution in the drinking water was determined using the blood cell count method.

After rearing in groups for two weeks (ten weeks old), mice in the sham group were sutured directly after opening the abdomen without ovariectomy. After opening the abdomen, mice in the OVX, LR+OVX, LA+OVX, and LR+LA+OVX groups were sutured to establish a menopausal OVX mouse model (Figure 1).

Mice continued to be housed in groups for six weeks (16 weeks of age) after surgery. Fecal samples were collected in cages (2 times/cage) from sixteen-week-old mice, transported and stored on dry ice, and sent to IGEbio in Guangzhou, China, to test the fecal microbial composition in mice. Eyeball blood collection was used to collect blood samples from each mouse, and ELISA was used to measure the levels of TNF- α , IL-6, OCN, and IL-1 β . After the execution of mice, mouse femur samples were obtained,

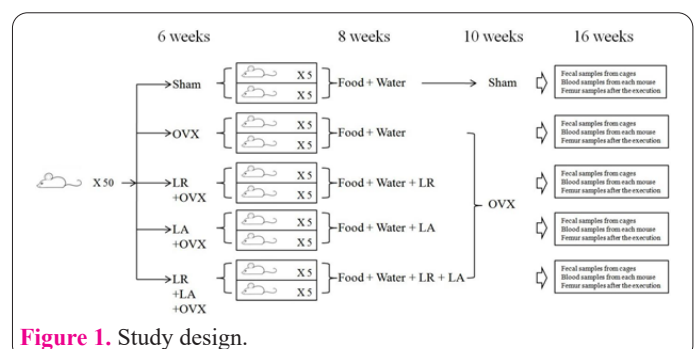


Figure 1. Study design.

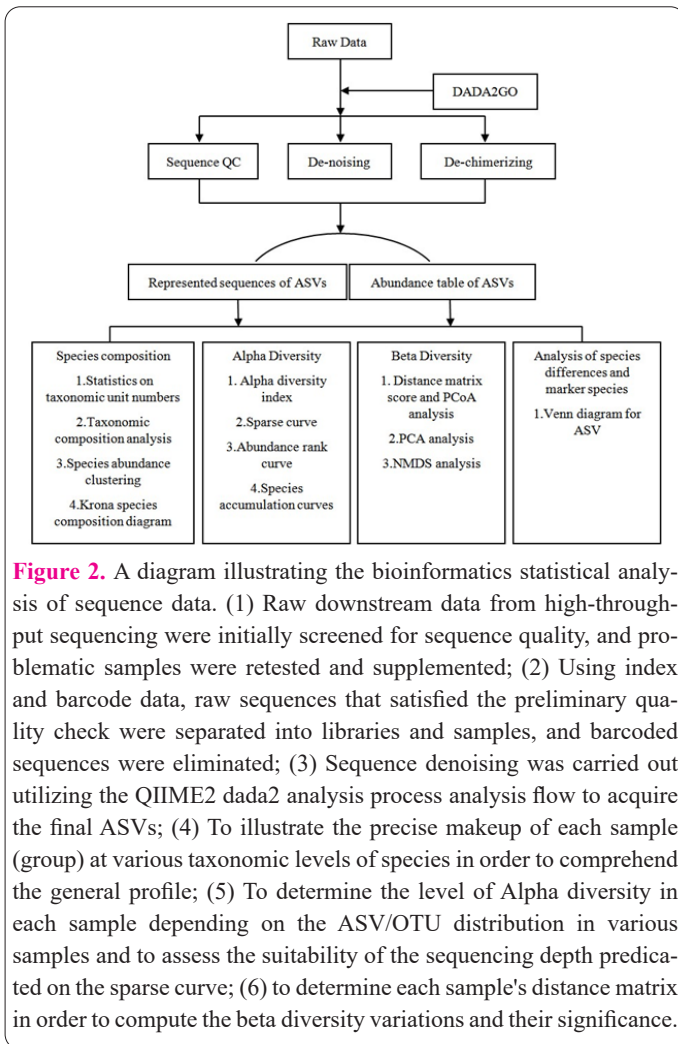


Figure 2. A diagram illustrating the bioinformatics statistical analysis of sequence data. (1) Raw downstream data from high-throughput sequencing were initially screened for sequence quality, and problematic samples were retested and supplemented; (2) Using index and barcode data, raw sequences that satisfied the preliminary quality check were separated into libraries and samples, and barcoded sequences were eliminated; (3) Sequence denoising was carried out utilizing the QIIME2 dada2 analysis process analysis flow to acquire the final ASVs; (4) To illustrate the precise makeup of each sample (group) at various taxonomic levels of species in order to comprehend the general profile; (5) To determine the level of Alpha diversity in each sample depending on the ASV/OTU distribution in various samples and to assess the suitability of the sequencing depth predicated on the sparse curve; (6) to determine each sample's distance matrix in order to compute the beta diversity variations and their significance.

and micro-CT scans were performed by 3D multi-model software to calculate the cortical thickness (Ct.Th), trabecular separation (Tb.Sp), trabecular thickness (Tb.Th), the trabecular number (Tb.N), and bone volume fraction (BV/TV) of mouse femurs (Figure 1).

The Dongguan People's Hospital's Laboratory Animal Welfare and Ethics Committee (Dongguan, China) approved the animal trials (No. IACUC-AWEC-202006001).

The menopausal OVX mouse model

Mice were injected intraperitoneally with 2.5% tri-bromoethanol (TBE) and operated prone after complete anesthesia. An incision of approximately 0.5 cm was made in the dorsal median of the third lumbar vertebrae bilaterally, the peritoneum was cut open, and the incision was explored with a tissue detector to locate the ovaries, which were ligated at the end of the fallopian tubes.

High-throughput sequencing and bioinformatics analysis of the fecal microbial composition

Barcoded 16S rDNA from microbial DNA is amplified by PCR for Illumina high-throughput sequencing. Amplified DNA is then sequenced using a high-throughput sequencer to obtain sequence information and understand the composition of microorganisms in mouse feces (Figure 2).

Mouse feces were collected in cages, and the Ipure Soil DNA Mini Kit (K3115-S, IGE Biologicals, Guangzhou, China) was used to recover bacterial DNA from the feces as per the package recommendations and refrigerated before

use at -80°C . The V4 high variant region of the prokaryotic 16S rDNA was chosen for amplification and further taxonomic analysis. The amplification was performed using primers 515F (5'-GTGYCAGCMGCCGCGGTAA-3') and 806R (5'-ggACTAC(A/g/C/T)(A/C/g)gggT(A/T)TC-TAAT-3') amplified the V4 high variant region from microbial genomic DNA. The PCR parameters were 94°C for 4 min, 94°C for 30 s, 58°C for 30 s (annealing), 72°C for 30 s (extension), and 72°C for 5 min (extension) for a total of 21 cycles. Illumina high-throughput sequence analysis (IGEbio, Inc., Guangzhou, China) was conducted on each $30\mu\text{g}$ purified PCR product. Raw data from the Illumina MiSeq platform were imported into GenBank (BioSample accession:KDDM00000000). Using a 97% criterion for sequence similarity, operational taxonomic units (OTUs) were clustered using the QIIME bioinformatics process, and the use of UCHIME facilitated the detection and elimination of chimeric sequences. The reads that were <2 and measuring <150 bp in length were removed. The final analysis was conducted utilizing the remaining sequences. With a confidence threshold of 0.8, the RDP Classifier (version 2.2) was applied to examine each 16S rDNA gene sequence's phylogenetic affinity against the SILVA database. Each library's taxonomic diversity and richness were assessed. To assess whether the sequencing depth was adequate to cover the anticipated number of OTUs, sparsity curves were generated. Non-metric multidimensional scaling analysis (NMDS) and principal component analysis (PCA) were conducted to distinguish between microbial communities.

Serum measurement

Blood samples from mice were collected by the eyeball extirpating method, after which they were given 1 hour of standing time at room temperature, followed by 10 minutes of centrifuging at 4,000 rpm. Before usage, the serum was extracted and preserved at -80°C . The Mouse OCN ELISA Kit (ml063317-C, mlbio, Shanghai China), the Mouse TNF- α ELISA Kit (ml002095-C, mBio, Shanghai, China), the Mouse IL-6 ELISA Kit (ml002293-C, mlbio, Shanghai, China), and the Mouse IL-1 β ELISA Kit (ml063132-C, mlbio, Shanghai, China) was utilized to quantify the serum OCN, TNF- α , IL-6, and IL-1 β concentrations as per the relevant guidelines.

micro-CT for bone density

The femurs were extracted bilaterally, the surrounding soft tissues and blood arteries were meticulously removed, and they were then submerged in paraformaldehyde after the execution of the experimental mice. Bilateral femur thin-layer scanning was performed utilizing a micro-CT (Siemens Invon) scanner (parameters used for imaging: magnification, $\times 6.7$; resolution, $30\mu\text{m}$; slice spacing, $240\mu\text{m}$; measurement time, 17 s; tube current, $88\mu\text{A}$; slice thickness, $240\mu\text{m}$; and tube voltage, 90 kV). The scanning area was the entire femur. The sample data for the following parameters were generated using 3D multi-model software after the scanning procedure: Ct.Th, Tb.Sp, Tb.Th, Tb.N, and BV/TV.

Statistical analysis

The serum and BMD findings were examined utilizing the statistical program SPSS 25.0. The two independent samples t-test was conducted to draw comparisons. $P <$

0.05 denoted the significance threshold. Alpha diversity analysis indexes were compared between groups using the ggpubr package in the R language for ANOVA statistical test analysis, and the criterion for significance was established at $P < 0.05$.

Results

Both LA and LR prevent bone loss in OVX mice

When mice were fed in groups up to 16 weeks of age, we took bilateral femurs of mice and used micro-CT (Siemens Invon) fourth in-layer scanning bilateral femurs to derive parameters related to bone volume in mice (Figure 3). The results showed a decrease in BV/TV, Tb.N, and Tb.Th respectively by 31%, 22%, and 14% in the OVX mice in contrast to the sham-operated group (Figures 4A, 4B, and 4C). Compared to the group that had a sham operation, the Tb.Sp rose by 47% (Figure 4D). The OVX mice fed with LA and LR experienced an increase in BV/TV, Tb.N, and Tb.Th (Figures 4A, 4B, and 4C), and the Tb.Sp decreased (Figure 4D). LR administration in OVX mice led to a 24% increase in BV/TV, a 16% increase in Tb.N, 9% increase in Tb.Th, and 22% decrease in Tb.Sp. The OVX mice fed LA had a 38% increase in BV/TV, a 28% increase in Tb.N, 9% increase in Tb.Th, and 31% decrease in Tb.Sp. LR and LA administration in OVX mice led to a 27% increase in BV/TV, an 18% increase in Tb.N, 8% increase in Tb.Th, and 24% decrease in Tb.Sp. However, no significant changes in the BV/TV, Tb.N, Tb.Th and Tb.Sp were observed in all probiotic feeding OVX mice (Figure 4A, 4B, 4C, and 4D). and no significant alterations in the Ct.Th were observed in all subgroups of mice (Figure 4E).

Both LA and LR reduce the expression of inflammatory factors in OVX mice

In mice fed until they were 16 weeks old, we evaluated the serum levels of inflammatory factors. The results showed that IL-6, TNF- α , and IL-1 β , as osteoclastogenic activators of bone metabolism, were elevated in OVX mice in contrast to the sham-operated group but not in OVX mice fed with LA (Figure 5A, 5B, 5C). As osteogenic activators of bone metabolism, OCN did not show statistically significant changes in grouped mice (Figure 5D). There was no statistical difference in inflammatory factors in OVX mice fed LA, LR, LA, and LR.

Altered GM in OVX mice after LA and LR feeding

The microbial composition of mouse feces was identified by Illumina high-throughput sequencing of the intes-

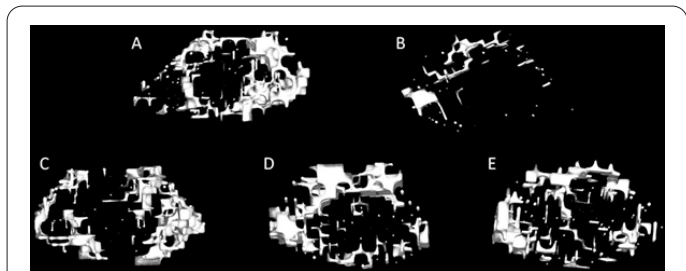


Figure 3. CT reconstruction of the lower segment of the femur in a mouse. (A) the sham group mouse. (B) the OVX group mouse. (C) the LR+OVX group mouse, (D) the LA+OVX group mouse, and (E) the LR+LA+OVX group mouse.

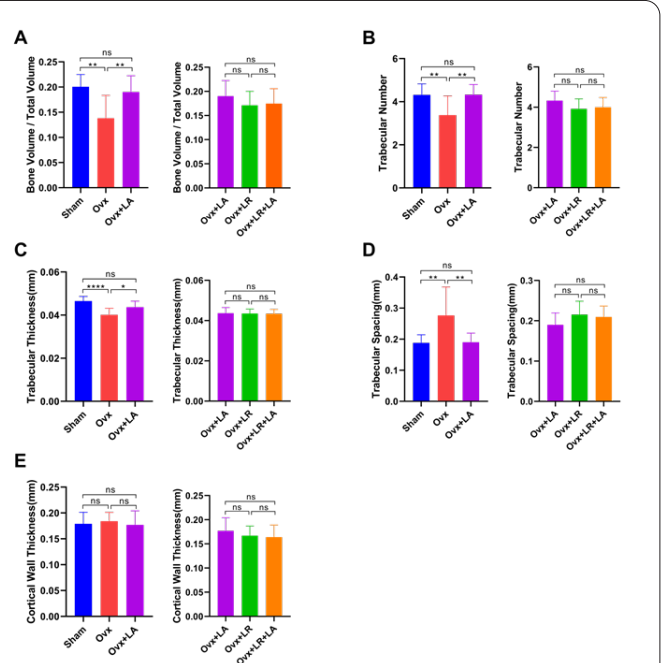


Figure 4. The bone volume fraction (BV/TV), the trabecular number (Tb.N), the trabecular thickness (Tb.Th), the trabecular separation (Tb.Sp), and the cortical thickness (Ct.Th) of mice were analyzed by micro-CT in both femurs. The independent samples t-test was utilized to compare the outcomes, which were displayed as mean \pm SEM, $n=10$, * $P < 0.05$, ** $P < 0.01$, *** $P < 0.0001$. (A, B) The BV/TV and Tb. N showed a substantial rise in the sham and LA+OVX groups in contrast to the OVX group. (C) The Tb.Th in the LA+OVX and sham groups significantly increased. (D) Comparing the OVX group to the sham and LA+OVX groups, the Tb.Sp was considerably higher in the former. (E) Comparing the OVX group to the LA+OVX and sham groups, the Ct. Th did not differ substantially.

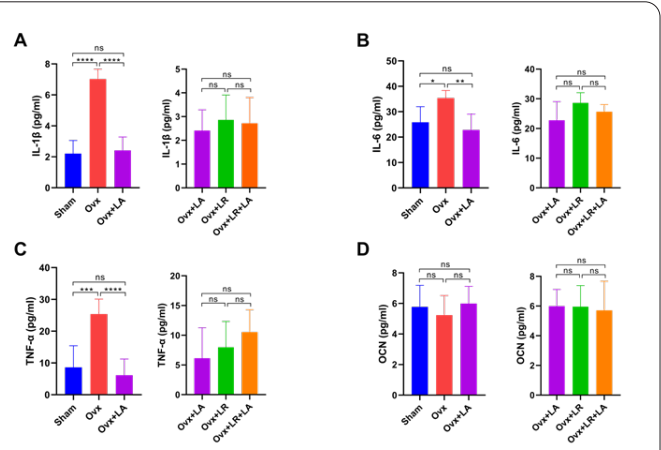


Figure 5. The serum levels of inflammatory factors in mice were detected by ELISA. The independent samples t-test was conducted to compare the outcomes, which were displayed as mean \pm SEM, $n=10$, * $P < 0.05$, ** $P < 0.01$, *** $P < 0.001$, **** $P < 0.0001$. (A, B, C) Comparing the OVX group to the sham and LA+OVX groups, IL-6, TNF- α , and IL-1 β levels were remarkably higher in the former. (D) The variation in OCN between the OVX group and the sham and LA+OVX groups was insignificant.

tinal microorganisms of each group of mice. By calculating the weighted unifracs distance by the Beta diversity analysis (Figure 6A), we observed differences between the gut microbial samples of all groups of mice. Changes in intestinal microorganisms were more pronounced in mice fed with probiotics than in the OVX group. On the contra-

Table 1. Fecal samples were collected from 16-week-old mice in cage units (ten mice per group housed in two cages, five mice per cage). To examine the microbial composition and characteristics, Illumina high-throughput sequencing was performed on mouse feces. S1_1, S1_2 represent the sham group, S2_1, S2_2 represent the OVX group, S3_1, S3_2 represent the LR+OVX group, S4_1, S4_2 represent the LA+OVX group, and S5_1, S5_2 represent the LR+LA+OVX group. Observed species: species count based on visual observations; the species population observed increases with index significance; Chao1 index: the species present in the community sample as a whole, the greater the Chao1 index, the less abundant the species are within the community; ACE index: the measure used to gauge how many OTUs are present in a community, the community richness increases as the ACE index increases. The Shannon index increases with an increase in community diversity and species distribution uniformity; Simpson: the diversity and uniformity of the species distribution in the community, where the Simpson index increases with species uniformity.

Sample	Observe	Chao1	ACE	Shannon	Simpson
S1_1	413	414.65	417.54	3.8173	0.94863
S1_2	467	474.13	479.66	3.8278	0.94861
S2_1	300	300.00	300.00	3.4285	0.93352
S2_2	297	297.00	297.00	3.41076	0.93283
S3_1	552	602.45	609.93	3.17556	0.88151
S3_2	585	635.16	642.56	3.19327	0.88323
S4_1	482	517.19	524.95	3.59424	0.93742
S4_2	509	586.77	580.27	3.6145	0.93881
S5_1	471	501.45	509.22	3.2312	0.90803
S5_2	523	575.16	572.18	3.2615	0.91039

Table 3. The richness of *Muribaculaceae* in the Bacteria domain by analyzing all intestinal microorganisms in the stool samples. The percentage of each species among all species was calculated. In the table, S1_1 and S1_2 represent the sham group, S2_1 and S2_2 denote the OVX group, S3_1 and S3_2 represent the LR+OVX group, S4_1 and S4_2 are the LA+OVX group, and S5_1 and S5_2 are the LR+LA+OVX group. It can be seen that the proportion of *Muribaculaceae* in the OVX, LR+OVX, LA+OVX, and LR+LA+OVX groups decreased in all species compared to the sham group.

	S1	S2	S3	S4	S5
1	26%	16%	5%	9%	8%
2	26%	16%	5%	9%	8%

Table 4. The richness of *Rikenellaceae* in the Bacteria domain was calculated by analyzing all intestinal microorganisms in fecal samples. The percentage of each species among all species was then calculated. In the table, S1_1 and S1_2 are for the sham group, S2_1, S2_2 for the OVX group, S3_1, S3_2 for the LR+OVX group, S4_1 and S4_2 are for the LA+OVX group, and S5_1 and S5_2 are for the LR+LA+OVX group. The proportion of *Rikenellaceae* in the LR+OVX group, LA+OVX group, and LR+LA+OVX group increased in all species compared to the sham group.

	S1	S2	S3	S4	S5
1	3%	1%	5%	6%	5%
2	3%	1%	5%	6%	5%

ry, there were no differences in mouse GM between groups receiving the same treatment. After performing the Alpha diversity index statistics, we found (Table 1, Figure 6B)) that the number of intestinal microorganisms in the OVX group had substantially fewer gut microbes in contrast to the sham-operated group. In contrast, the probiotic-fed OVX mice had more gut microbes. By comparing the Chao1 and ACE indices, we observed a decrease in the richness of gut microorganisms and a decrease in low-richness species in the OVX group. Probiotic-fed OVX mice showed an increase in richness and an increase in low-abundance species. By comparing the Shannon and Simpson indices, we observed that OVX mice with or without probiotic feeding recorded a reduction in homogeneity in contrast to sham surgery.

In the analysis of the taxonomic composition of the intestinal microorganisms of each group of mice, we found that at the phylum level (Figure 7A), in contrast, the richness of *Bacteroidetes* in the intestinal microorganisms of all OVX mice was reduced in contrast to the sham-operated

group. Furthermore, the richness of *Firmicutes* increased whereas that of *Verrucomicrobiota* decreased in the OVX group. Conversely, the LR+OVX group experienced a decrease in the richness of *Firmicutes* and an increase in *Verrucomicrobiota*. Moreover, the LA+OVX group had a decrease in the richness of *Firmicutes* and an increase in *Proteobacteria*. The richness of *Verrucomicrobiota* increased in the LR+LA+OVX group. At the order level, *Erysipelotrichales*:*Lactobacillales* were remarkably higher in the OVX group than in the probiotic group (Figure 7B). The increase in the richness of *Proteobacteria* in the LA+OVX group was mainly due to a significant increase in the richness of *Enterobacteriales* (Table 2, Figure 7C). The richness of *Bacteroidetes* was reduced in intestinal microorganisms in all OVX mice, and there was a decrease in the richness of *Enterobacteriaceae*, primarily manifested by the reduction of *Muribaculaceae* (Table 3). However, at the family level, there was a slight increase in the richness of *Rikenellaceae* in mice fed with probiotics (Table 4).

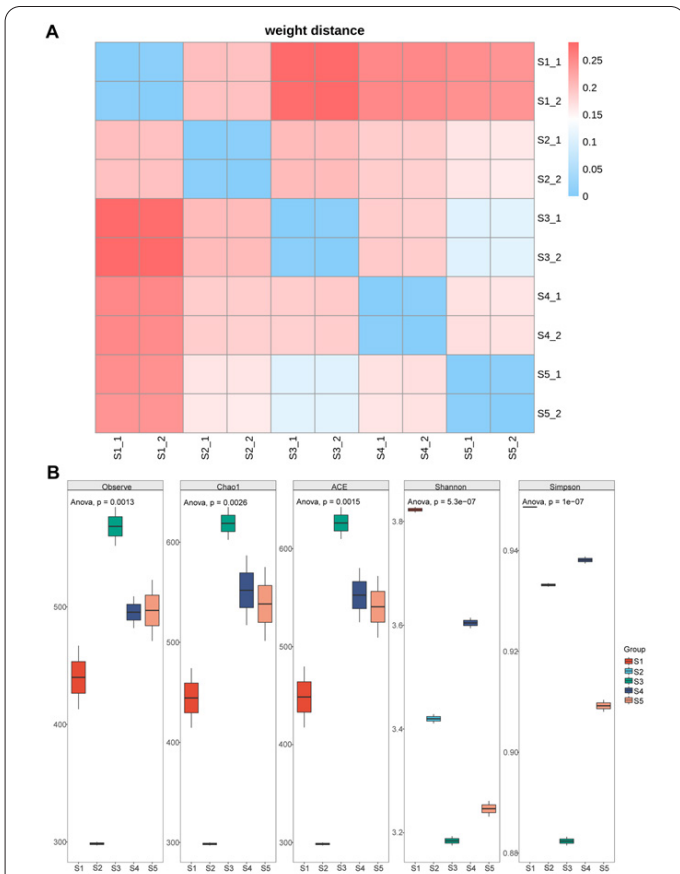


Figure 6. (A) The dissimilarity coefficient between the two samples was calculated in the Beta diversity study using the weighted unifracs distance. The weighted unifracs considers both the presence or absence of species change and species richness and as the value decreases, the species diversity difference between these two samples decreases as well. In the Figure, S1_1 and S1_2 denote the sham group, S2_1 and S2_2 represent the OVX group, S3_1 and S3_2 denote the LR+OVX group, S4_1 and S4_2 illustrate the LA+OVX group, and S5_1 and S5_2 denote the LR+LA+OVX group. The weighted unifracs distance between the sham group and LR+OVX group, LA+OVX group, and LR+LA+OVX group was more significant than the distance between the sham and OVX groups. In contrast, the weighted unifracs distance of intestinal microorganisms of mice within each group was 0. (B) S1 represents the sham group, S2 represents the OVX group, S3 represents the LR+OVX group, S4 represents the LA+OVX group, and S5 represents the LR+LA+OVX group. The results were compared using the ggpubr package for ANOVA statistical test analysis in the R language. Differences in observed Chao1, ACE, Shannon, and Simpson indexes between the groups were statistically significant at $P < 0.05$.

Discussion

Probiotics and prebiotics have a positive therapeutic effect on osteoporosis. The most common probiotics used for intervention are *L.rhamnosus GG*(LGG), LR, *L.paracasei*, *L.plantarum*, *L.bulgaricus*, and *Lactococcus lactis*. Probiotics include xylooligosaccharides (XOS), fructooligosaccharides(FOS), glucomannans, and acid-hydrolyzed high amylose corn starch (AH-HAS)(26). Bone loss in ovariectomized rat models can be ameliorated by single or multiple probiotic feeding combinations(27). Prebiotics mixed with probiotics or fermented can also be used to enhance calcium absorption and anti-osteoporosis effect(28). By lowering osteoclast bone resorption indicators and activators (Trap5 and RANKL), LR reduces the OVX-mediated upregulations in bone marrow CD4+T

cells (which enhance osteoclastogenesis) and directly suppresses osteoclastogenesis *in vitro*. Additionally, LR altered the microbial community in the gut of OVX mice to prevent bone loss (14). LR prevents glucocorticoid-triggered bone loss in mice by reducing prednisolone-induced apoptosis of osteoblasts and osteocytes(29). Reduced osteoblast and increased osteoclast activity were observed in antibiotic-induced ecological dysregulation. LR prevented bone loss in antibiotic mice by modulating GM(18). LGG prevents bone loss in mice deficient in sex steroids by reducing intestinal permeability and inhibiting inflammation of the intestinal and bone marrow(30). LGG prevents TDF (tenofovir disoproxil fumarate)-induced bone loss in mice by reconstituting the microbial structure, promoting the expression of lysophosphatidylcholine (LPC), improving intestinal integrity (integrity), and suppressing the inflammatory response(31). FOS and glucomannans prevented SAMP6 (senescence-accelerated mouse prone 6)-induced bone losses by altering the GM (significantly higher amounts of *Lactobacillus* and *Bacteroides*) and reducing the systemic inflammatory response(32). Resistant starch (RS) increased the richness of *Bifidobacterium* spp. in the feces, upregulated the expression levels of colonic IL-10 mRNA in OVX mice, and downregulated the expression of myeloid nuclear factor kappa-B receptor activator ligand and IL-7 receptor genes to prevent bone loss (33).

Postmenopausal osteoporosis is a systemic inflamma-

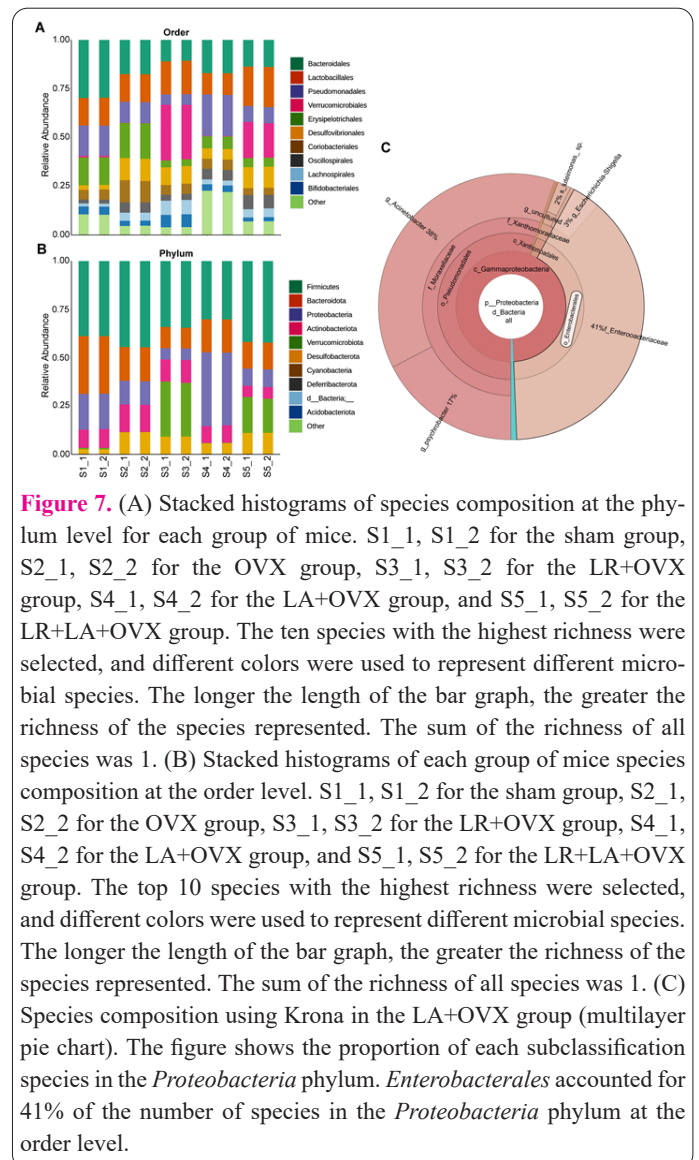


Figure 7. (A) Stacked histograms of species composition at the phylum level for each group of mice. S1_1, S1_2 for the sham group, S2_1, S2_2 for the OVX group, S3_1, S3_2 for the LR+OVX group, S4_1, S4_2 for the LA+OVX group, and S5_1, S5_2 for the LR+LA+OVX group. The ten species with the highest richness were selected, and different colors were used to represent different microbial species. The longer the length of the bar graph, the greater the richness of the species represented. The sum of the richness of all species was 1. (B) Stacked histograms of each group of mice species composition at the order level. S1_1, S1_2 for the sham group, S2_1, S2_2 for the OVX group, S3_1, S3_2 for the LR+OVX group, S4_1, S4_2 for the LA+OVX group, and S5_1, S5_2 for the LR+LA+OVX group. The top 10 species with the highest richness were selected, and different colors were used to represent different microbial species. The longer the length of the bar graph, the greater the richness of the species represented. The sum of the richness of all species was 1. (C) Species composition using Krona in the LA+OVX group (multilayer pie chart). The figure shows the proportion of each subclassification species in the *Proteobacteria* phylum. *Enterobacteriales* accounted for 41% of the number of species in the *Proteobacteria* phylum at the order level.

tory response regulated by immune factors(34). In mouse models, estrogen deficiency increases intestinal permeability in the small intestine and bone mass, expands Th17 cells, and upregulates the osteoclast factor TNF- α (30). Histamine produced by LR inhibits the TNF- α signaling pathway by modulating PKA and ERK signaling(35). A study by Ohlsson et al. noted that LR treatment remarkably lowered the serum levels of IL-6, TNF- α , and IL-1 β (17). However, probiotic treatment did not significantly affect serum OCN(14, 17). Treatment with *Lactobacillus* downregulated the expression levels of two inflammatory factors, TNF- α and IL-1 β , in the cortical bone of OVX mice. However, *Lactobacillus* also failed to elevate serum OCN levels in normal and OVX mice, suggesting that probiotic treatment did not affect bone formation(17). LA was found to provide the same bone loss prevention effect in OVX mice as LR. The expression of osteoclast activators IL-6, TNF- α , and IL-1 β in the serum of OVX mice decreased after feeding LR and LA. In OVX mice, osteoclast signaling pathway activation was suppressed. Tb.N, Tb.Th, BV/TV, and Tb. Sp did not vary significantly in OVX mice as a result, and neither did Tb. Sp. Unfortunately, Ct.Th did not produce differences between the groups. We speculate that this may be related to the absence of a significant elevation of OCN in the serum of OVX mice, in which case the osteogenic pathway was not activated.

Previously, Britton et al. found that the intestinal microbial richness was significantly higher in mice treated with LR 6475 than in untreated mice(14). Li et al. reported that glucocorticoid treatment resulted in decreased bone mineral density and decreased diversity index (Shannon index) and richness index (Chao1 index) of gut microorganisms. On the contrary, the bone density, richness, and diversity indices were restored after the application of CC (CaCO₃) and TBP (tuna bone powder) (36). Our results suggest that the number of intestinal microbial species, their richness (ACE index), and the number of low-abundance species (Chao1 index) might perform a positive function in preserving bone mass. In contrast, the homogeneity of species distribution (Shannon index) may have little relationship with the preservation of bone mass. This suggests that an increase in some species-specific gut microorganisms would reduce evenness and thus have a protective or destructive effect on bone mass.

We can also see from the weighted unifracs distance that OVX mice showed a more significant change in their gut microbial diversity after probiotic feeding. Some changes in the GM of OVX mice also occurred after different probiotic feeding. This suggests that the gut microorganisms that are protective against bone mass are also diverse. The similarities lie in the fact that different probiotic feeds lead to an increase in inflammatory factors that activate osteoclasts in bone metabolism. There are two possible reasons for this. One is that some bacteria in the gut microbes of the OVX mice fed probiotics dominate this process, and the other is that the increased diversity of the gut microbes activates some mechanism that causes this process. We also found no variability in GM in mice treated with the same treatment method. This indicates that the changes in intestinal microorganisms in mice with the same treatment method have a pattern and consistency.

The composition of intestinal microorganisms in mice is dominated by *Firmicutes* and *Bacteroidetes*(4). Schep- peret al. showed that the reduction in femoral trabecular

bone mass of mice by about 30% after the application of antibiotics might be associated with an increase in *Firmicutes:Bacteroidetes* ratio (18). In another study, the richness of *Firmicutes* was increased in the GM mice treated with subtherapeutic doses of antibiotics (37). In another study by Schepperet al., glucocorticoid-treated mice had reduced bone mass and lower *Bacteroidetes* richness in gut microbes(29). Tousenet al. found that OVX mice fed with dietary fiber supplementation of RS attenuated ovariectomy-induced reduction of *Bacteroides* in intestinal microbes(33). Our experiments revealed that with or without probiotics, all OVX mice showed a significant reduction in the richness of *Bacteroidetes* in intestinal microorganisms and an increase in *Firmicutes:Bacteroidetes* compared to sham surgery. The richness of *Firmicutes* increased in the OVX group, whereas it decreased in the LR+OVX and LA+OVX groups. We suggest that the increase in *Firmicutes* richness and the decrease in *Bacteroidetes* richness may be related to bone loss. By further comparing multiple OTUs, we found that *Erysipelotrichales* and *Lactobacillales* were essential components of *Firmicutes*. Additionally, the bone loss resulting from elevated *Firmicutes* could be remarkably linked to the increase in order levels of *Erysipelotrichales:Lactobacillales*. Among *Bacteroidetes*, *Rikenellaceae* did not decrease but increased after probiotic application, which may be an observable indicator to assess beneficial effects on bone mass after probiotic application in OVX mice.

Although *Firmicutes:Bacteroidetes* increased and *Bacteroidetes* richness decreased in the LR+OVX and LA+OVX groups in contrast to the sham-operated group, the bone loss in the mice was insignificant, suggesting that there were other gut microorganisms in the experimental group that played a protective role against bone loss. A significant increase in the richness of *Verrucomicrobiota* was observed in the LR+OVX and LR+LA+OVX groups in contrast to the sham-operated group. Conversely, a decrease in the richness of *Verrucomicrobiota* occurred in the OVX group. Consistent with the findings of Schepperet al., the richness of *Verrucomicrobiales* in the intestinal microbiota of mice to which glucocorticoids were applied also showed a decrease (29). We suggest that the increase in the richness of *Verrucomicrobiales* may be related to the preservation of bone mass. The richness of *Proteobacteria* appeared significantly higher in the LA+OVX group as opposed to the sham-operated and OVX groups. At the level of order in *Proteobacteria*, *Enterobacteriales* were significantly increased. In experiments studying the application of LGG for the treatment of osteoporosis caused by TDF (Tenofovir disoproxil fumarate), the richness of *Enterobacteriales* was relatively higher in the mice to which LGG was applied(31). This may indicate that the increase in *Enterobacteriales* has a protective effect on bone mass.

Similarly, in a study of intestinal microbes in postmenopausal patients with osteoporosis, it was possible to find a decrease in the index of intestinal microbial diversity, a decline in the abundance of the *Bacteroidetes* phylum, and an increase in the abundance of *Lactobacillales* in the *Firmicutes* characterized(5). This is the same result that we observed under the OVX mouse model. However, the index of intestinal microbial diversity was surprisingly increased in postmenopausal patients with reduced bone mass as opposed to the normal group, with an increase in the phylum of *Proteobacteria* (*Proteobacteria*) (5). This

is consistent with the performance of the OVX mice after the LA application. We think this may be a self-protective mechanism in humans before developing postmenopausal osteoporosis. Notably, the diversity index of gut microorganisms was increased in patients with primary osteoporosis. The abundance of the *Bacteroidetes* phylum (*Bacteroides*) increased, and the abundance of *Erysipelotrichales* in *Firmicutes* decreased (7). This is in contrast to changes characterized by intestinal microbes in OVX mice and postmenopausal osteoporosis patients. This may suggest that the approach of altering gut microbes by applying probiotics alone may not be applicable to primary osteoporosis. It has also been shown that bone density in elderly patients with osteoporosis is not associated with microbiota diversity but with altered biota abundance(38). The pattern of figuring out BMD by looking at intestinal microbes may not be the same for all types of osteoporotic patients.

In conclusion, *L. acidophilus* positively affected *L. reuteri* in preventing bone loss in de-ovalized mice. The mechanism of action may be that by inhibiting the activation of inflammatory factors in the osteoclast activation pathway in bone metabolism, the diversity of GM is regulated, and the abundance of microorganisms is altered, leading to the attenuation of bone loss. The difference is that LA varies from LR in that it can influence the richness of a particular microorganism. This implies that there could be variations in the mechanism probiotics protect against bone loss in OVX mice via modulating GM. Our investigation offers further proof for the additional exploration of probiotics in the treatment of postmenopausal osteoporosis and offers new ideas for diagnosing osteoporosis using gut microbial analysis. However, studies have still not identified clear gut microbial targets to accurately elucidate the specific changes in gut microbes at various stages during the development of osteoporosis. In future studies, we can explore the changes in gut microbes and inflammatory factors at different stages of osteoporosis to further elucidate the relationship.

Acknowledgements

The authors are grateful to Charles River (Beijing, China) for providing us with mice. We thank Jennio Biotech (Guangzhou, China) for providing a place to feed and operate our mice. Thanks to Guangdong Institute of Microbiology (Guangdong Microbiological Analysis and Testing Center) for providing us with probiotics. The authors thank IGEbio (Guangzhou, China) for testing the fecal microbial composition in mice.

Interest conflict

The authors declare that they have no competing interests.

Consent for publications

The author read and proved the final manuscript for publication.

Availability of data and material

All data generated during this study are included in this published article.

Authors' Contribution

(I) Conception and design: JCC, XYL; (II) Administrative support: XYL, SBL; (III) Provision of study materials or

patients: JCC, JWL; (IV) Collection and assembly of data: JCC, JWL; (V) Data analysis and interpretation: JCC, JWL; (VI) Manuscript writing: All authors; (VII) Final approval of manuscript: All authors.

Funding

This study was funded by Dongguan Social Science and Technology Development Project (grant no. 201950715001202). The design of the study, the collection and interpretation of the data, the analysis of the results, and the writing of the manuscript were carried out by the authors in our hospital. However, none of this would have been possible without the financial support of the funding agency.

References

1. Dennison E, Cole Z, Cooper C. Diagnosis and epidemiology of osteoporosis. *Curr Opin Rheumatol* 2005; 17(4):456-461.
2. Chen P, Li Z, Hu Y. Prevalence of osteoporosis in China: a meta-analysis and systematic review. *BMC Public Health* 2016; 16(1):1039.
3. Kanis JA, Cooper C, Rizzoli R, et al. European guidance for the diagnosis and management of osteoporosis in postmenopausal women. *Osteoporos Int* 2019; 30(1):3-44.
4. Nguyen TL, Vieira-Silva S, Liston A, Raes J. How informative is the mouse for human gut microbiota research? *Dis Model Mech* 2015; 8(1):1-16.
5. He J, Xu S, Zhang B, et al. Gut microbiota and metabolite alterations associated with reduced bone mineral density or bone metabolic indexes in postmenopausal osteoporosis. *Aging (Albany NY)* 2020; 12(9):8583-8604.
6. Li C, Huang Q, Yang R, et al. Gut microbiota composition and bone mineral loss-epidemiologic evidence from individuals in Wuhan, China. *Osteoporos Int* 2019;30(5):1003-1013.
7. Xu Z, Xie Z, Sun J, et al. Gut Microbiome Reveals Specific Dysbiosis in Primary Osteoporosis. *Front Cell Infect Microbiol* 2020;10:160.
8. Zaiss MM, Jones RM, Schett G, Pacifici R. The gut-bone axis: how bacterial metabolites bridge the distance. *J Clin Invest* 2019;129(8):3018-3028.
9. Quach D, Britton RA. Gut Microbiota and Bone Health. *Adv Exp Med Biol* 2017; 1033:47-58.
10. Vemuri RC, Gundamaraju R, Shinde T, et al. Therapeutic interventions for gut dysbiosis and related disorders in the elderly: antibiotics, probiotics or faecal microbiota transplantation? *Benef Microbes* 2017; 8(2):179-192.
11. Sánchez B, Delgado S, Blanco-Míguez A, et al. Probiotics, gut microbiota, and their influence on host health and disease. *Mol Nutr Food Res* 2017; 61(1).
12. Markowiak P, Śliżewska K. Effects of Probiotics, Prebiotics, and Synbiotics on Human Health. *Nutrients* 2017; 9(9).
13. Van den Nieuwboer M, Brummer RJ, Guarner F, et al. The administration of probiotics and synbiotics in immune compromised adults: is it safe? *Benef Microbes* 2015; 6(1):3-17.
14. Britton RA, Irwin R, Quach D, et al. Probiotic *L. reuteri* treatment prevents bone loss in a menopausal ovariectomized mouse model. *J Cell Physiol* 2014; 229(11):1822-1830.
15. Collins FL, Rios-Arce ND, Schepper JD, et al. Beneficial effects of *Lactobacillus reuteri* 6475 on bone density in male mice is dependent on lymphocytes. *Sci Rep* 2019; 9(1):14708.
16. Collins FL, Irwin R, Bierhalter H, et al. *Lactobacillus reuteri* 6475 Increases Bone Density in Intact Females Only under an Inflammatory Setting. *PLoS One* 2016; 11(4):e0153180.

17. Ohlsson C, Engdahl C, Fak F, et al. Probiotics protect mice from ovariectomy-induced cortical bone loss. *PLoS One* 2014; 9(3):e92368.
18. Schepper JD, Collins FL, Rios-Arce ND, et al. Probiotic *Lactobacillus reuteri* Prevents Postantibiotic Bone Loss by Reducing Intestinal Dysbiosis and Preventing Barrier Disruption. *J Bone Miner Res* 2019; 34(4):681-698.
19. Jones ML, Martoni CJ, Prakash S. Oral supplementation with probiotic *L. reuteri* NCIMB 30242 increases mean circulating 25-hydroxyvitamin D: a post hoc analysis of a randomized controlled trial. *J Clin Endocrinol Metab* 2013; 98(7):2944-2951.
20. Montazeri-Najafabady N, Ghasemi Y, Dabbaghmanesh MH, et al. Supportive Role of Probiotic Strains in Protecting Rats from Ovariectomy-Induced Cortical Bone Loss. *Probiotics Antimicrob Proteins* 2019; 11(4):1145-1154.
21. Nilsson AG, Sundh D, Backhed F, et al. *Lactobacillus reuteri* reduces bone loss in older women with low bone mineral density: a randomized, placebo-controlled, double-blind, clinical trial. *J Intern Med* 2018; 284(3):307-317.
22. Bull M, Plummer S, Marchesi J, et al. The life history of *Lactobacillus acidophilus* as a probiotic: a tale of revisionary taxonomy, misidentification and commercial success. *FEMS Microbiol Lett* 2013; 349(2):77-87.
23. Farag MA, El Hawary EA, Elmassry MM. Rediscovering acidophilus milk, its quality characteristics, manufacturing methods, flavor chemistry and nutritional value. *Crit Rev Food Sci Nutr* 2020; 60(18):3024-3041.
24. Paul AK, Paul A, Jahan R, et al. Probiotics and Amelioration of Rheumatoid Arthritis: Significant Roles of *Lactobacillus casei* and *Lactobacillus acidophilus*. *Microorganisms* 2021; 9(5).
25. Scriven M, Dinan TG, Cryan JF, et al. Neuropsychiatric Disorders: Influence of Gut Microbe to Brain Signalling. *Diseases* 2018; 6(3):78.
26. Li J, Ho WTP, Liu C, et al. The role of gut microbiota in bone homeostasis. *Bone Joint Res* 2021; 10(1):51-59.
27. Gholami A, Dabbaghmanesh MH, Ghasemi Y, et al. The ameliorative role of specific probiotic combinations on bone loss in the ovariectomized rat model. *BMC Complement Med Ther* 2022; 22(1):241.
28. Zhou J, Cheng J, Liu L, et al. *Lactobacillus acidophilus* (LA) Fermenting Astragalus Polysaccharides (APS) Improves Calcium Absorption and Osteoporosis by Altering Gut Microbiota. *Foods* 2023; 12(2):275.
29. Schepper JD, Collins F, Rios-Arce ND, et al. Involvement of the Gut Microbiota and Barrier Function in Glucocorticoid-Induced Osteoporosis. *J Bone Miner Res* 2020; 35(4):801-820.
30. Li JY, Chassaing B, Tyagi AM, et al. Sex steroid deficiency-associated bone loss is microbiota dependent and prevented by probiotics. *J Clin Invest* 2016; 126(6):2049-2063.
31. Liu H, Gu R, Li W, et al. *Lactobacillus rhamnosus* GG attenuates tenofovir disoproxil fumarate-induced bone loss in male mice via gut-microbiota-dependent anti-inflammation. *Ther Adv Chronic Dis* 2019; 10(2040622319860653).
32. Tanabe K, Nakamura S, Moriyama-Hashiguchi M, et al. Dietary Fructooligosaccharide and Glucomannan Alter Gut Microbiota and Improve Bone Metabolism in Senescence-Accelerated Mouse. *J Agric Food Chem* 2019; 67(3):867-874.
33. Tousein Y, Matsumoto Y, Nagahata Y, et al. Resistant Starch Attenuates Bone Loss in Ovariectomised Mice by Regulating the Intestinal Microbiota and Bone-Marrow Inflammation. *Nutrients* 2019; 11(2):297.
34. Weitzmann MN, Pacifici R. Estrogen deficiency and bone loss: an inflammatory tale. *J Clin Invest* 2006; 116(5):1186-1194.
35. Thomas CM, Hong T, van Pijkeren JP, et al. Histamine derived from probiotic *Lactobacillus reuteri* suppresses TNF via modulation of PKA and ERK signaling. *PLoS One* 2012; 7(2):e31951.
36. Li J, Yang M, Lu C, et al. Tuna Bone Powder Alleviates Glucocorticoid-Induced Osteoporosis via Coregulation of the NF- κ B and Wnt/ β -Catenin Signaling Pathways and Modulation of Gut Microbiota Composition and Metabolism. *Mol Nutr Food Res* 2020; 64(5):e1900861.
37. Cho I, Yamanishi S, Cox L, et al. Antibiotics in early life alter the murine colonic microbiome and adiposity. *Nature* 2012; 488(7413):621-626.
38. Das M, Cronin O, Keohane DM, et al. Gut microbiota alterations associated with reduced bone mineral density in older adults. *Rheumatology (Oxford)* 2019; 58(12):2295-2304.